https://doi.org/10.48048/tis.2022.2996

Graphite Exfoliation using MnO_2 Paste via Sonication in Irradiated Water for Volumetric-Shrinkage Resistant Sponge

Wipsar Sunu Brams Dwandaru[1,2,*], Fika Fauzi[1,2], Suparno[1], Supardi[1], Athi' Nur Auliati Rahmah[1], Buky Wahyu Pratama[3], Rhyko Irawan Wisnuwijaya[1] and Emi Kurnia Sari[3]

[1]Department of Physics Education, Faculty of Mathematics and Natural Sciences, Universitas Negeri Yogyakarta, Yogyakarta, Indonesia
[2]Research Center for Sustainable Nanomaterials, Universitas Negeri Yogyakarta, Yogyakarta, Indonesia
[3]Department of Physics, Faculty of Mathematics and Natural Sciences, Universitas Gadjah Mada, Yogyakarta, Indonesia

([*]Corresponding author's e-mail: wipsarian@uny.ac.id)

Received: 8 November 2020, Revised: 22 May 2021, Accepted: 31 May 2021

Abstract

Graphite exfoliation has been the main mechanism to produce graphene material and its derivatives, such as graphene oxide (GO) and reduced GO (rGO). This study was aimed to exfoliate graphite using MnO_2 paste in Zinc-Carbon (ZnC) battery wastes via audio sonication in X-ray irradiated water. The exfoliated graphite (EG) sample was then characterized using UV-Vis spectrophotometry, FTIR spectroscopy, XRD, and SEM. The EG sample was utilized as an additive for producing sponge with heat-induced volumetric-shrinkage resistance property. The irradiated water was obtained by exposing X-ray radiation upon distilled water. The graphite and K_2MnO_4 were mixed in the irradiated water followed by audio sonication accompanied by stirring and heating. The K_2MnO_4 was obtained from the MnO_2 paste added with KOH. The UV-Vis results showed a shouldering peak at 271 nm indicating that the graphite was succesfully exfoliated. The FTIR test showed the presence of hydroxyl, C-O, CO_2, N-O, and C=C functional groups. The XRD showed a peak at 12° for the EG sample similar to the XRD peak of GO. The SEM images showed layers of graphene flakes. The threshold temperature values of the sponge, sponge with EG (sponge+EG), and sponge with graphite (sponge+graphite) were 399.20, 271.03, and 414.82 °C, respectively. The sponge+EG underwent less volume shrinkage compared to ordinary sponge and sponge+graphite, which confirms its volume shrinkage resistant upon heating.

Keywords: Graphite exfoliation, Resistant sponge, Water irradiation, Audio sonication

Introduction

Graphene and its derivatives, e.g. graphene oxide (GO) and reduced-GO (rGO) are nanomaterials that are being intensively developed. Many studies are conducted to produce these materials to become more specific and functional. Many applications of graphene include electronics, bio-sensor, and hydrogen transfers [1,2]. The methods in the synthesis of graphene and its derivatives that are often utilized include Hummer's method, liquid sonication exfoliation (LPE), and chemical vapor deposition (CVD) [3-5]. A commonly used method in producing graphene and/or its derivative is the Hummer's method, which uses many chemicals such as K_2MNO_4, MnO_2, KOH, and HCl [6-8]. Hence, this method may be harmful to the environment, especially when chemical wastes are produced after the production process.

More specifically, GO synthesis using X-ray irradiation and audio sonication exposure methods have also been conducted [9,10]. X-ray irradiation upon (pure) water is called radiolysis [11], whereas the audio sonication method uses sound wave in audio frequency range i.e. 20 Hz to 20 kHz, which is exposed to a graphite sample dispersed in detergent. This method does not employ as many chemicals as in the Hummer's method so it can be considered environmentally friendly. In addition, this method is convenient to do and can be conducted only in a few hours. Hence, this method can be used as an inexpensive and environmentally friendly alternative to mass-produce GO materials. On the other hand, the radiolysis of water produces various radicals, i.e. hydrated electrons, hydrogen radical (H*), hydroxyl

radical (HO*), HO_2*, OH^-, H_3O^+, H_2, and hydrogen peroxide (H_2O_2). Moreover, these radicals are very reactive and may recombine into superoxide (HO_2) and peroxide (H_2O_2). Although the lifetime of these radicals are very short (nanosecond scale), their effect upon the water remains. Hence, HO_2 and H_2O_2 molecules assist the exfoliation of the graphene layers in the graphite material oxidized by K_2MNO_4. Moreover, it is also argued that ions produced, such as OH^- and H_3O^+ may interact with the graphite material in between the graphene layers, hence increasing the intercalation of the graphene layers.

Sponge is a substance that has pores or cavities. There are three forms of sponge, which is hard, medium, and soft. Each form has different applications such as sound-absorbent, dishwashers, heat-resistant coatings (insulators), impact absorbent, seat and housing materials, and hydroponics [12-17]. In general, the sponge base material is polyurethane (PU), which consists of two types of liquids, namely PU A and B, respectively [18]. PU A is an ingredient for compacting the sponge, whereas PU B is the ingredient for sponge development. Many studies have been conducted concerning GO-based sponge. Zhang *et al*. [19] conducted a study on chitosan/GO-based sponge to reduce its toxicity obtaining sponges with excellent absorption capacity, mechanical stability, and bio-compatibility. Xu *et al.* [20] had produced GO wide ribbon (GOWR) based sponges, which is sensitive to abnormally high temperature of 300 °C for early warning fire alarm [20]. However, the sponge itself has not been tested for its volume-shrinkage resistance induced by heating. Testing the sponges by heating them may determine their mechanical volume-shrinkage and even heat-resistance properties [21]. This is important in the application of sponges for heat-resistant kitchen appliances and costumes to increase the safety of people who use appliances for cooking, conduct dangerous fire stunts, and car racing.

The objective of this study was to synthesize exfoliated graphite (EG) dispersed in K_2MnO_4 solution via audio sonication in X-ray irradiated water. The graphite powder was dispersed in the K_2MnO_4 solution obtained from the MnO_2 paste in Zinc-Carbon (ZnC) battery wastes. The MnO_2 is one of the main components in this ZnC battery [22], which can be transformed into K_2MnO_4 solution by addition of KOH through the reaction given as follows;

$$4\mathrm{KOH}\,(s) + 2\mathrm{MnO_2(s)} + \mathrm{O_2}(g) \leftrightarrows 2\mathrm{K_2MnO_4}(s) + 2\mathrm{H_2O}\,(l). \quad (1)$$

The resultant sample was then used as an additive material for producing sponge (sponge+EG) with heat-induced volume-shrinkage resilience property. The sponge+EG is then heated in an oven to test its volume-shrinkage resilience by measuring its volume as the temperature is increased.

Materials and methods

The materials used in this study were 1) graphite powder, 2) distilled water, 3) PU foams (A and B), 4) KOH, and 5) MnO_2 from ZnC battery wastes. The tools used in this study were 1) X-ray generator, 2) audio frequency generator (AFG), iii) amplifiers, 4) loudspeaker, and 5) hot plate magnetic stirrer. The audio sonicator and the magnetic stirrer were combined into a custom-made device, which can be observed in **Figure 1**.

K_2MnO_4 was synthesized according to the procedure given as follows. 65 g of KOH were mixed with 50 g of MnO_2. Then the solution was heated and stirred simultaneously for 15 min. The K_2MnO_4 solution was synthesized based on the chemical reaction given in Eq. (1).

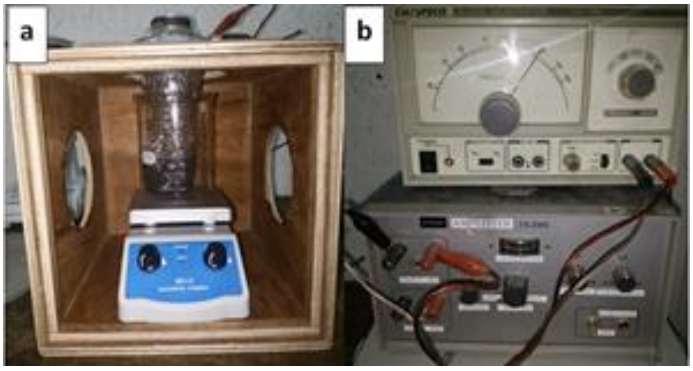

Figure 1 The devices used consisting of a) a magnetic stirrer, and b) an AFG (b-top), and an amplifier (b-bottom).

Figure 2 The sample of the EG powder.

The EG sample was prepared as follows. 200 mL of distilled water was irradiated using the X-ray generator for 2 h at 20 kV. 100 mL of the irradiated water was then used to mix 2 g of graphite powder and 0.5 g of K_2MnO_4 using a magnetic stirrer for 15 min. Subsequently, audio sonication was exposed to the sample with a frequency of 100 Hz accompanied by stirring and heating using a magnetic stirrer at 60 °C for 2 h. This process caused the water in the sample to dry out, hence turning the sample into powder as observed in **Figure 2**.

The samples obtained were then characterized using UV-Visible spectrophotometer (UV-Vis), Fourier transform infrared (FTIR), X-ray diffraction (XRD), and scanning electron microscope (SEM). UV-Vis and FTIR characterizations were conducted in liquid phase, whereas XRD and SEM were conducted in powder form. The liquid phase of the sample was obtained by dissolving the powder into 100 mL of distilled water. The procedure of the experiment may be observed in **Figure 3**.

The sponges were prepared according to the following steps. 0.5 g of the EG powder was mixed with 5 mL of PU A and 10 mL of PU B. The mixing was done using a magnetic stirrer for 1 min. The mixture was then poured into a molded container, left to expand and harden to form a sponge+EG in 15 min. The same procedure above was also conducted to produce sponge with graphite (sponge+graphite), meanwhile ordinary sponge was prepared from a mixture of PU A and PU B only.

The heat-resistance characterization of the sponges was conducted by heating the sponge samples inside an oven and measuring the volume of the sponges as the temperature of the oven was varied, i.e. 100, 150, 200 and 250 °C. The volume was determined via measurements of the length, width, and height of the sponges using a caliper. The volume was obtained by multiplying the length, width, and height. To obtain the threshold temperature values of the sponge samples, i.e. sponge+EG, sponge+graphite, and sponge, the extrapolation using the linear trend line function in MS Excel was utilized.

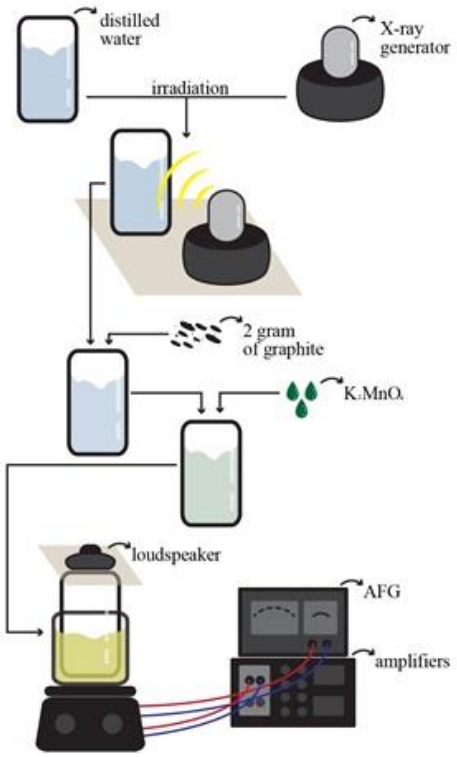

Figure 3 The procedure in the exfoliation of graphite.

Results and discussion

The UV-Vis spectrum of the EG compared to the original graphite is presented in **Figure 4**. The solid-blue line is the EG showing a broad-weak absorbance peak at 271 nm. The typical absorbance peaks for GO commonly appear around 230 nm and a shouldering peak at 300 nm [23,24]. The rGO absorbance peak at around 270 nm is usually strong and sharp [25-27], but here a weak and quite broad peak is obtained, which indicates that the graphite is exfoliated. Moreover, the UV-Vis spectrum of EG is in contrast to the graphite UV-Vis spectrum given by the dashed-red line, which shows no absorbance peak. It can be concluded that the oxidation process due to K_2MnO_4 on the graphite leads to the exfoliation of the graphite layers. The radiolysis water affects the readiness of exfoliation process of the graphite sample. Thus, after sonication, the EG sample becomes more graphene-like with reduced oxygen indicated by the absorption in 271 nm.

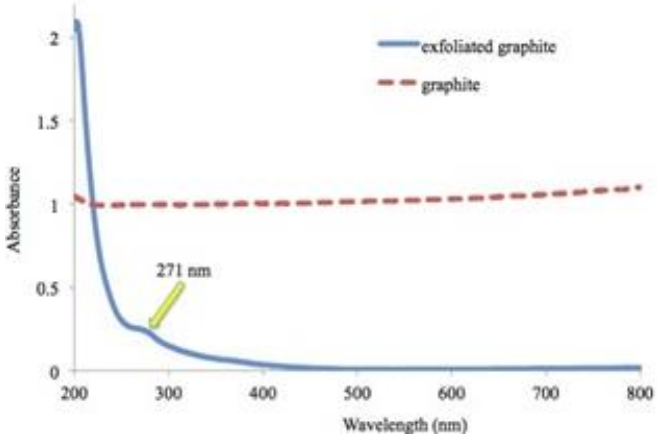

Figure 4 The UV-Vis of EG compared to the original graphite.

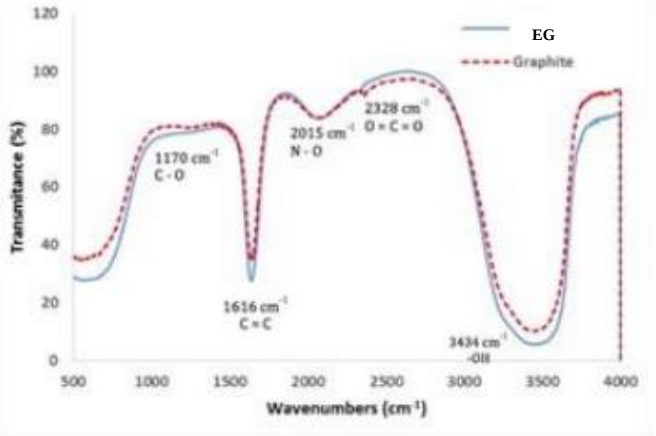

Figure 5 FTIR spectra of EG and graphite samples.

The FTIR spectrum of the EG sample compared to the original graphite is presented in **Figure 5**. Both spectra indicate the presence of bands at 3434, 2328, 2015, 1616 and 1170 cm^{-1}, which correspond to the functional groups of hydroxyl (OH), carbon dioxide (O=C=O), N-O, C=C, and C-O, respectively. It may be observed that the oxygen functional groups have weak bands, except for the usual hydroxyl functional groups. It can be observed that the existence of C=C and oxygen functional groups confirm the formation of EG as well as graphite samples. This is because the C=C functional group contains in both EG and graphite materials. However, it may be observed that the band of the OH functional group of the EG material is wider than graphite. Moreover, this is similar to the FTIR spectrum obtained in [28] especially for the functional groups of hydroxyl, carbon dioxide, C=C, and C-O at 3434.59, 2362.78, 1627.64 and 1084.17 cm^{-1}, respectively.

The diffractogram of the EG sample compared to graphite is shown in **Figure 6**. Both of the XRD patterns exhibit a broad 2θ of around 10 - 20° that may be caused by the sample holder of the XRD apparatus, which commonly occurs in the characterization process. It can be observed that the strongest peak for graphite is around 2θ of 26.5°, while the strongest peak for the EG sample appears at 2θ of around 12°, apart from the broad band due to the sample holder. The peak at 26.5° indicates the presence of (002) plane of hexagonal lattice of graphite, which correlates with the stacking layers of graphene in the graphite sample. This peak disappears in the EG spectrum, which indicates that the graphite was exfoliated due to the sonication process in the radiolysis water and K_2MnO_4 solution. The EG spectrum at around 12° is related to the crystal plane of (001) from the hexagonal lattice of few layers of graphite. The evolution of XRD pattern from graphite into GO indicates the structural change of graphite in terms of the number of layers and the distance among graphite planes. This is in accordance with the XRD data for GO, which is generally around 10º and suggests the stacking of GO sheets [29-31].

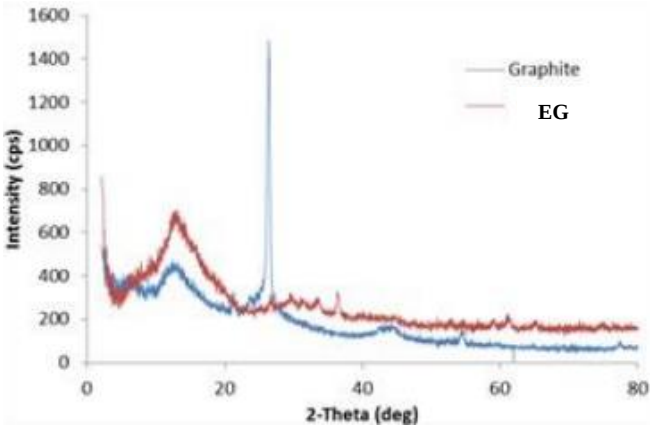

Figure 6 XRD spectra of EG and graphite samples.

Finally, **Figure 7** shows the SEM images of a) graphite and b) EG materials. The SEM images show the surface morphology of the graphite and EG samples with magnification of 5000X. The SEM image of the EG material (**Figure 7(b)**) shows few layers stacking of graphene flakes, which tend to be thinner than that of graphite material (**Figure 7(a)**). Furthermore, it can be observed in the red box in **Figure 7(b)** that the surface of the EG material has crack lines and wrinkles indicating the thinness of the layers. Due to the thinness of its surface, the EG material tend to agglomerate and tend to be more wrinkled than the graphite surface. In addition, this feature is due to the EG's surface-to-volume ratio, which is higher than that of the graphite material. This surface structure of the EG is in accordance with the study in [32].

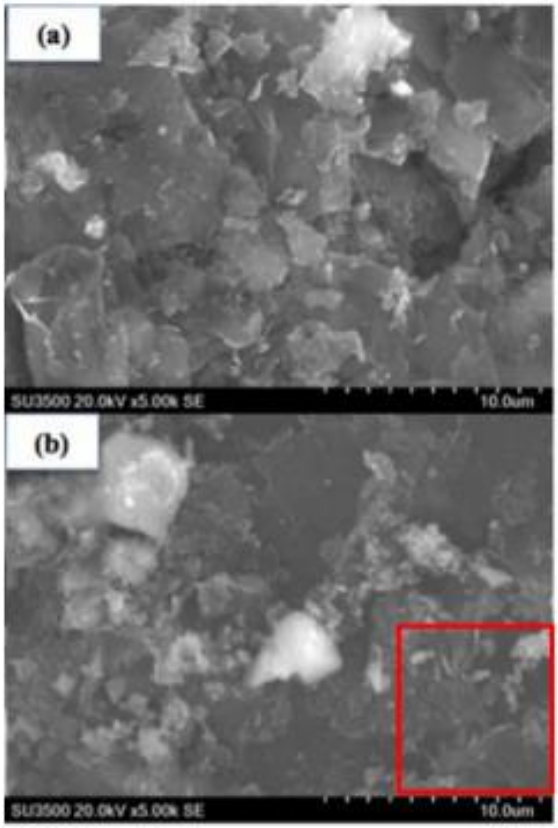

Figure 7 SEM images with 5000X magnification of (a) graphite, and (b) EG samples.

The results of the addition of graphite and EG to sponges can be observed in **Figure 8**. The Figure shows the sponges produced with different ingredients, i.e. sponge+EG (**Figure 8(a)**), ordinary sponge (**Figure 8(b)**), and sponge+graphite (**Figure 8(c)**). There is a clear difference in colour between the 3 sponge samples. The sponge+EG, sponge, and sponge+graphite tend to be white with black spots, yellowish, and darkish, respectively. This indicates that mixing different materials into the sponge affects the colour of the sponge itself. The clear yellow colour of the ordinary sponge is caused by the chemical nature of the material being mixed. In addition, in this case graphite and EG are originally made from carbon materials producing different colour on the mixing process of the sponge.

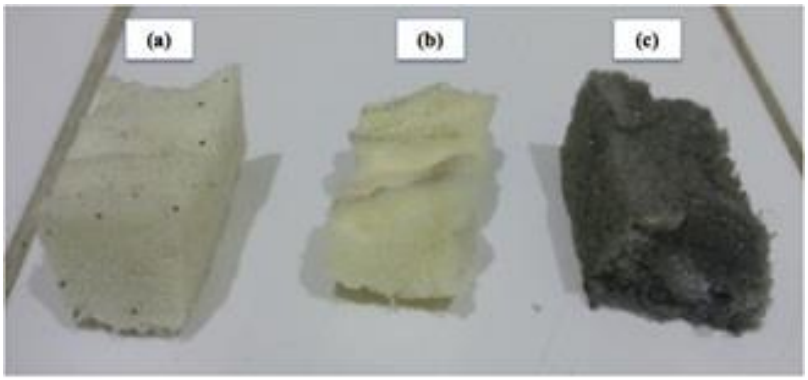

Figure 8 Physical appearance of (a) sponge+EG, (b) sponge, and (c) sponge+graphite.

As previously discussed, these sponge samples are heated in the oven and their volumes are measured as the temperature of the oven is increased. The results of the sponge heating tests can be observed in **Figure 9**. The Figure shows various sponge samples, namely sponge+EG, ordinary sponge, and sponge+graphite exposed to heating temperature from 100 to 250 °C (see yellow arrow going down from **Figures 9(a)** to **9(e)**). It may be observed that all sponge samples undergo volume shrinkage as the temperature of the oven is increased. However, qualitatively, the sponge+EG sample has the least volume shrinkage at 250 °C. It can also be observed that each temperature increase changes the colour of each sample. The sponge+EG still has a brighter colour compared to the ordinary sponge and sponge+grahite. The ordinary sponge and sponge+graphite samples tend to have dark colour, while sponge+EG is still light brown at 250 °C. Moreover, it can be observed that the volume of sponge+EG sample tends to be stable - because the reduction in volume is not too significant as the temperature is increased. This is clearly different from the ordinary sponge sample, which undergoes a slight increase at 150 °C and then starts to shrink drastically when passing 150 °C towards 250 °C. This indicates that sponge+EG can maintain its volume against high temperatures.

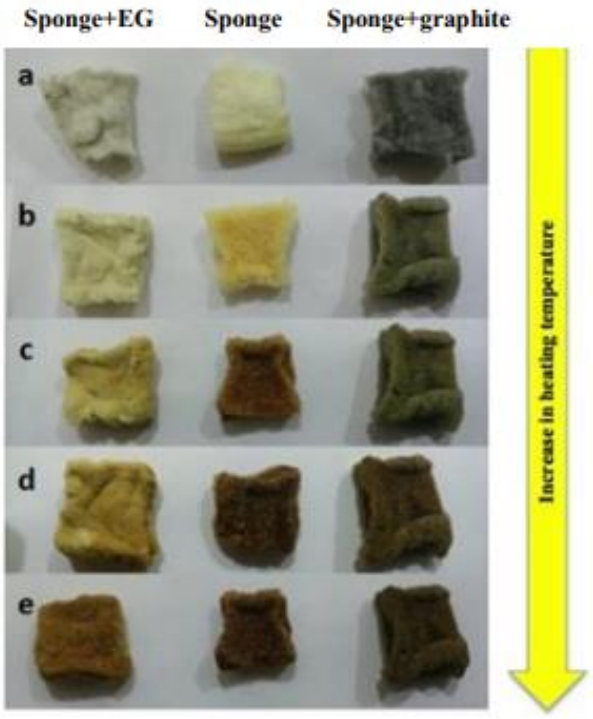

Figure 9 Heating results of the sponge samples with temperature variations at a) room temperature, b) 100 °C, c) 150 °C, d) 200 °C, and e) 250 °C.

In addition, the trend line graphs of the sponge samples may be observed in **Figure 10**. It is clearly observed that the ordinary sponge sample increases its volume under heating until around 150 °C, and then shrinks beyond it. This is different with sponge+EG and sponge+graphite, which suffer linear volume shrinkage under heating. However, the sponge+graphite is more rapidly decreasing compared to the sponge+EG sample. This confirms that sponge+EG sample is more resistant to volume shrinkage compared to ordinary sponge. The threshold temperatures of the ordinary sponge, sponge+graphite, and sponge+EG are 399.20, 414.82, and 1271.03 °C, respectively. From this data it is found that the volume of the sponge+EG will hypothetically be 0 when the temperature reaches 1271.03 °C, which is the highest temperature value compared to sponge+graphite and ordinary sponge samples. Hence, adding EG results in the increase of volume resistant of the sponge to more than 200 % compared to ordinary sponge. It is worth noting that this threshold temperature for 0 volume only gives a qualitative picture of the sponge's volume shrinkage that goes beyond the data points [33].

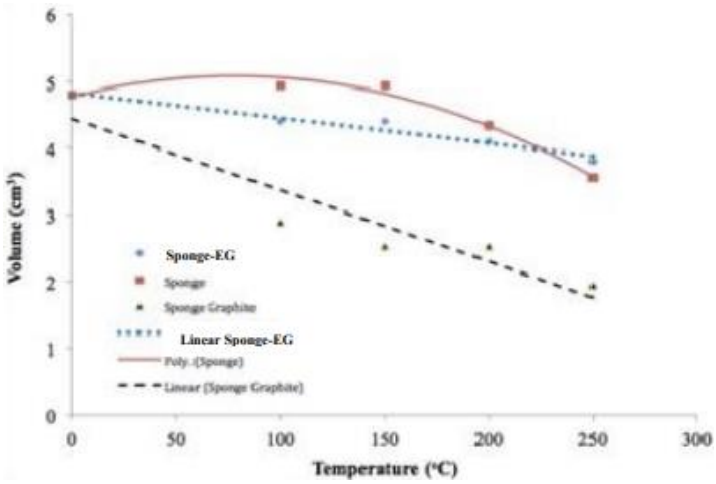

Figure 10 The volume shrinkage graphs of the sponge samples.

Conclusions

EG material has been produced based on the UV-Vis, FTIR, XRD, and SEM characterization results. The EG material is obtained by dispersing graphite and K_2MnO_4 solution in X-ray irradiated water assisted by audio sonication and heating. The heat induced volume-shrinkage resistance test results show that sponge+EG sample has the least volume reduction compared to ordinary sponge and sponge+graphite. Further study upon the EG sample includes determining the flakes size based on the SEM results. It is interesting to test other properties of the sponge+EG, e.g. its compressive strength, which can be conducted in future studies.

Acknowledgements

We would like to thank the Faculty of Mathematics and Natural Sciences, Universitas Negeri Yogyakarta, Indonesia for funding this research through the Research Group scheme of 2019.

References

[1] B Zhan, C Li, J Yang, G Jenkins, W Huang and X Dong. Graphene field-effect transistor and its application for electronic sensing. *Small* 2014; **10**, 4042-65.

[2] Z Khan, TR Chetia, AK Vardhaman, D Barpuzary, CV Sastri and M Qureshi. Visible light assisted photocatalytic hydrogen generation and organic dye degradation by CdS-metal oxide hybrids in presence of graphene oxide. *RSC Adv.* 2012; **2**, 12122-8.

[3] B Paulchamy, G Arthi and BD Lignesh. A simple approach to stepwise synthesis of graphene oxide nanomaterial. *J. Nanomed. Nanotechnol.* 2015; **6**, 1000253.

[4] A Ciesielski and P Samorì. Graphene via sonication assisted liquid-phase exfoliation. *Chem. Soc. Rev.* 2014; **43**, 381-98.

[5] X Li, L Colombo and RS Ruoff. Graphene films: Synthesis of graphene films on copper foils by chemical vapor deposition. *Adv. Mater.* 2016; **28**, 6247-52.
[6] S Chen, J Zhu, X Wu, Q Han and X Wang. Graphene oxide-MnO_2 nanocomposites for supercapacitors. *ACS Nano* 2010; **4**, 2822-30.
[7] K Noiroj, P Intarapong, A Luengnaruemitchai and S Jai-In. A comparative study of KOH/Al_2O_3 and KOH/NaY catalysts for biodiesel production via transesterification from palm oil. *Renew. Energ.* 2009; **34**, 1145-50.
[8] A Alighardashi, Kashitarash, Z Esfahani and F Najafi. Efficiency evaluation of nitrate removal from synthetic solution by dendrimer-graphene oxide nano-composite activated with HCl. *J. Water Wastewater* 2019; **30**, 101-6
[9] WSB Dwandaru, BW Pratama, RI Wisnuwijaya, LD Parwati, DS Khaerudini, Supardi and Suparno. Mixing of graphite with x-ray irradiated water towards the exfoliation of graphene layers. *Nanosci. Nanotechnol. Asia* 2020; **10**, 548-56.
[10] WSB Dwandaru, LD Parwati and RI Wisnuwijaya. Formation of graphene oxide from carbon rods of zinc-carbon battery wastes by audiosonic sonication assisted by commercial detergent. *Nanotechnol. Precis. Eng.* 2019; **2**, 89-94.
[11] SL Caer. Water radiolysis: Influence of oxide surfaces on H_2 production under ionizing radiation. *Water* 2011; **3**, 235-53.
[12] PM Fernández, RLJ Cruz, LE García-Cambronero, C Díaz and MA Navacerrada. García-Cambronero, C Díaz and MA Navacerrada. Sound absorption properties of aluminium sponges manufactured by infiltration process. *Adv. Mater. Res.* 2010; **146-147**, 1651-4.
[13] M Sharma, J Eastridge and C Mudd. Effective household disinfection methods of kitchen sponges. *Food Contr.* 2009; **20**, 310-3.
[14] S Jiang, B Uch, S Agarwal and A Greiner. Ultralight, thermally insulating, compressible polyimide fiber assembled sponges. *ACS Appl. Mater. Interfac.* 2017; **9**, 32308-15.
[15] AM Lazim, DL Musbah, CC Chin, I Abdullah, MHA Mustapa and A Azfaralariff. Oil removal from water surface using reusable and absorptive foams via simple fabrication of liquid natural rubber (LNR). *Polym. Test* 2019; **73**, 39-50.
[16] S Kovačević and D Ujević. *Seams in car seat coverings: Properties and performance*. *In*: I Jones and GK Stylios (Eds.). Joining textiles principle and applications. Woodhead Publishing, Sawston, United Kingdom, 2013, p. 478-506.
[17] NAS Helal. Studies of different germination media and package on squash and snake cucumber sprouts. *Middle East J. Appl. Sci.* 2016; **6**, 374-8.
[18] D Zhao, Z Zhao, X Dai, S Wang, S Liu and Y Liu. Study on mechanical properties of a novel polyurethane sponge magnetorheological elastomers in compressive mode. *Mater. Res. Express* 2019; **6**, 116101.
[19] Y Zhang, J Guan, J Wu, S Ding, J Yang, J Zhang, J Zhang, A Dong and L Deng. N-alkylated chitosan/graphene oxide porous sponge for rapid and effective hemostasis in emergency situations. *Carbohydr. Polym.* 2019; **219**, 405-13.
[20] H Xu, Y Li, NJ Huang, ZR Yu, PH Wang, ZH Zhang, QQ Xia, LX Gong, SN Li, L Zhao, GD Zhang and LC Tang. Temperature-triggered sensitive resistance transition of graphene oxide wide-ribbons wrapped sponge for fire ultrafast detecting and early warning. *J. Hazard. Mater.* 2019; **363**, 286-94.
[21] H Wang, X Zhang, N Wang, Y Li, X Feng, Y Huang, C Zhao, Z Liu, M Fang, G Ou, H Gao, X Li and H Wu. Ultralight, scalable, and high-temperature-resilient ceramic nanofiber sponges. *Sci. Adv*. 2017; **3**, e1603170.
[22] SM Shin, G Senanayake, JS Sohn, JG Kang, DH Yang and TH Kim. Separation of zinc from spent zinc-carbon batteries by selective leaching with sodium hydroxide. *Hydrometallurgy* 2009; **96**, 349-53.
[23] M Bera, C Yadav, P Gupta and PK Maji. Facile one-pot synthesis of graphene oxide by sonication assisted mechanochemical approach and its surface chemistry. *J. Nanosci. Nanotechnol.* 2018; **18**, 902-12.
[24] N Pan, D Guan, T He, R Wang, I Wyman, Y Jin and C Xia. Removal of Th^{4+} ions from aqueous solutions by graphene oxide. *J. Radioanal. Nucl. Chem.* 2013; **298**, 1999-2008.
[25] R Krishna, E Titus, O Okhay, JC Gil, J Ventura and EV Ramana. Rapid electrochemical synthesis of hydrogenated graphene oxide using ni nanoparticles. *Int. J. Electrochem. Sci.* 2014; **9**, 4045-69.

[26] MK Rabchinskii, VV Shnitov, AT Dideikin, AE Aleksenskii, SP Vul, MV Baidakova, II Pronin, DA Kirilenko, PN Brunkov, J Weise and SL Molodtsov. Nanoscale perforation of graphene oxide during photoreduction process in the argon atmosphere. *J. Phys. Chem. C* 2016; **120**, 28261-69.
[27] Y Zhang, W Hu, B Li, C Peng, C Fan and Q Huang. Synthesis of polymer-protected graphene by solvent-assisted thermal reduction process. *Nanotechnology* 2011; **22**, 345601-6.
[28] Sudesh, N Kumar, S Das, C Bernard and GD Varma. Effect of graphene oxide doping on superconducting properties of bulk MgB_2. *Supercond. Sci. Tech.* 2013; **26**, 095008.
[29] FT Johra, JW Lee and WG Jung. Facile and safe graphene preparation on solution based platform. *J. Ind. Eng. Chem.* 2014; **20**, 2883-7.
[30] R Siburian, H Sihotang, S Raja, Lumban, M Supeno and C Simanjuntak. New route to synthesize of graphene nano sheets. *Orient. J. Chem.* 2018; **34**, 182-7.
[31] ACD Moraes, BA Lima, AFD Faria, M Brocchi and OL Alves. Graphene oxide-silver nanocomposite as a promising biocidal agent against methicillin-resistant *Staphylococcus aureus. Int. J. Med.* 2015; **10**, 6847-61.
[32] F Fauzi, F Azizi, MM Musawwa and WSBD Dwandaru. Synthesis and characterizations of reduced graphene oxide prepared by microwave irradiation with sonication. *J. Phys. Sci*. 2021; **32**, 1-13.
[33] J Franklin. Arguments whose strength depends on continuous variation. *J. Informal Logic* 2013; **33**, 33-56.